Soft Matter

Concepts, Phenomena, and Applications

Short section on Flocking

Wim van Saarloos
Vincenzo Vitelli
Zorana Zeravcic

Princeton University Press
Princeton and Oxford

identifies the symmetries of the building blocks and the appropriate order parameter for the relevant collective phases, very much as in passive matter. Figure 9.1 illustrates this with four examples that we will encounter in this chapter.

Such so-called Janus particles are typically made by coating one side of the colloid with a catalyst for a reaction that takes place in the fluid; see figure 4.18. Figure 4.19 shows various examples of rod-like active particles which tend to align.

The first experimental system, illustrated in the top row of figure 9.1, is composed of colloids that can self-propel in a given direction at a certain speed. In the presence of orientation-aligning interactions the colloids tend to move along a common direction; the proper order parameter is therefore a polar vector.

Well-known examples of molecular motors are kinesin and myosin. For more information, see section 3.6.2 and the illustrations of molecular motors in figure 3.11 and figure 3.12.

The second example illustrated in the figure concerns biopolymers, such as microtubules or actin filaments, with molecular motors that apply force dipoles along the direction in which they are oriented. On large scales, this mixture can exhibit nematic order described by the vector order parameter of liquid crystals, the director $\hat{n}$ introduced in section 6.1.4. If the particles are, however, self-propelled in a direction that undergoes a random walk without alignment (similarly to bacteria that run and tumble), density is the appropriate *scalar* order parameter, as illustrated in the third example.

The final example concerns so-called living crystals made of embryos, volvox algae, or driven colloids that constantly spin instead of self-propel. In this case, a tensor order parameter describing strains is needed to describe the system, as in ordinary solids. In addition, one could also add a field describing the local spinning rate of the particles $\Omega(r, t)$ in the hydrodynamic description.

Throughout this chapter we will use the order parameter description to discuss the hydrodynamics equations that capture the microscopic source of activity relevant to all of these models.

9.2 Flocking

Figure 9.2. A flock of birds. Albert Beukhof/Shutterstock. Schools of fish similarly exhibit coordinated movement.

Flocking is perhaps the most paradigmatic example of collective behavior in active matter systems. Active constituents, like flying birds, self-organize into complex patterns over length scales which are very large compared to the size of a bird, see figure 9.2. Within the flock, nearby birds fly in the same average direction, while on large scales the average flight orientation typically varies. In this section, we will see how traditional physics approaches can be used to construct a rich explanatory framework to model flocking.

9.2.1 The Vicsek model

Flocking can be described within a simplified setting usually referred to as the Vicsek model.[3] This model makes a drastic

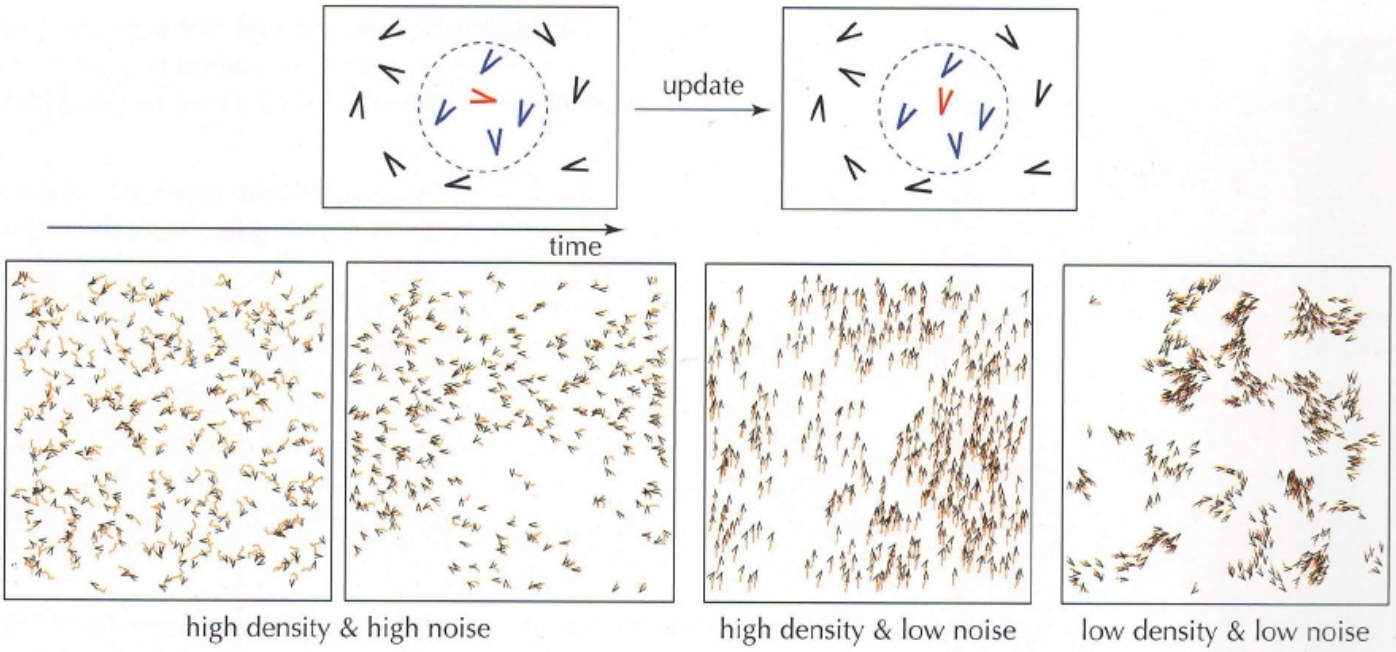

Figure 9.3. Left: in the Vicsek model the direction of the velocity of the red bird particle in the center of the dashed circle is updated to be the average orientation of all particles within that circle (the red and blue ones), plus a random noise term. The four snapshots of simulations of the Vicsek model for various densities and noise strengths on the right illustrate that flocking occurs for low noise strength.[1] For small densities and noise the particles form flocks which move in random directions, while for large densities and small noise an ordered phase emerges with all particles moving on average in the same direction. Adapted from Vicsek et al., 1995[2].

simplification and views a flock of birds as a set of particles which in each time step move a fixed distance forward in the direction in which they are oriented. However, their flight direction is updated in each time step to become equal to the average orientation of the birds within some finite range R plus noise, as illustrated on the left side of figure 9.3.

At www.complexity-explorables.org/ you can play with simulations of the Vicsek model. The website contains many other instructive examples of complex systems, including one called *Flock'n Roll*.

In the two-dimensional Vicsek model, each particle is characterized by the position $\vec{r}_i$ and θ_i, where θ_i is the orientation angle of particle i with respect to some fixed axis. The update rule for the positions and angles of the particles is

$$\begin{aligned} \vec{r}_i(t+\Delta t) &= \vec{r}_i(t) + v_0 \Delta t \begin{pmatrix} \cos\theta_i(t) \\ \sin\theta_i(t) \end{pmatrix}, \\ \theta_i(t+\Delta t) &= \langle\theta(t)\rangle_{R,i} + \eta_i(t), \end{aligned} \tag{9.1}$$

with v_0 denoting a characteristic self-propulsion speed, Δt the characteristic time between steps, and the average angle defined as

$$\langle\theta(t)\rangle_{R,i} \equiv \arg\left(\sum_j e^{i\theta_j(t)}\right), \tag{9.2}$$

where the index j runs over all particles within some distance R from the particle i. For simplicity we take $\Delta t = 1$. The term η_i represents a stochastic noise and is assumed to be uncorrelated

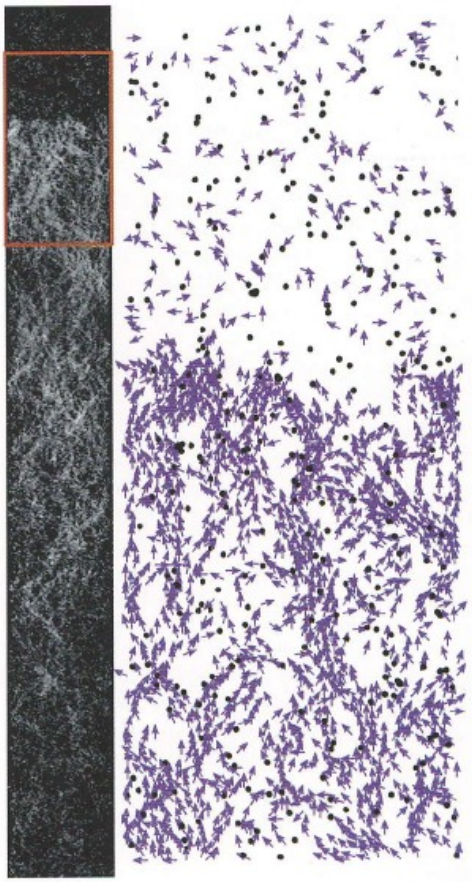

Figure 9.4. Observation by Morin et al., 2016 of collective motion of colloidal particles in a long channel with small random obstacles. Left: global view. The channel contains 8,500 colloids, and it is 7 mm long and about 850 microns wide. The active motion is due to Quincke rotation, illustrated in figure 4.19(e). The right-hand image shows an enlargement of the flocking front in the area indicated by a red box in the left-hand image, with arrows indicating the velocity orientation. Black dots indicate the obstacles used in these experiments to probe the behavior of flocking fronts in a random environment. A sharp density front is clearly visible. Quincke rotation experiments provide a versatile soft matter realization for studying flocking as well as studying front, band, and vortex formation.[5] Image courtesy of Denis Bartolo.

The argument in this section is inspired by the lecture notes of Toner, 2018; see also the review by Vicsek and Zafeiris, 2012.

between particles and between different update times,[4]

$$\overline{\eta_i(t)} = 0, \qquad \overline{\eta_i(t)\eta_j(t')} = 2\gamma\,\delta_{ij}\delta_{tt'}. \tag{9.3}$$

Figure 9.3(b) illustrates the behavior of the model for various densities and noise strengths. For large noise strength, the birds tend to fly mostly in random directions. But for small noise strength, when they have a strong tendency to align with their neighbors, they tend to form flocks. For small densities (upper right snapshot) the birds cluster in flocks which move in random directions, while for large densities all birds tend to fly on average in the same direction. These snapshots are indicative of what has emerged from many detailed studies, namely that the model exhibits three phases, a disordered, an ordered homogeneous, and an ordered banded phase in which the bird density is spatially modulated.

Intuitively, it is rather easy to understand why the model has a tendency to form flocks with relatively sharp boundaries. The update rule favors birds in a dense region flying on average in the same direction, making escaping a flock difficult. Moreover, once a lonely bird in an empty region happens to fly into a flock, it tends to adjust its flight orientation almost immediately to join the flock. In other words, there is a strong tendency in the model for the particles to separate into dense flocks and relatively low density regions.

Flocking behavior of the type seen in such simulations has been observed and studied in detail in a variety of active matter systems. Figure 9.4 shows this for the case of active colloids driven by the Quincke rotation mechanism illustrated in figure 4.19.d.

We will not go into the details of phase diagram and scaling properties of the Vicsek model here[6] but will concentrate on the continuum formulations which capture the essence of the behavior, while providing a good starting point for including additional effects.

9.2.2 Flocking and the Mermin-Wagner theorem

Before we embark on our discussion of phenomenological equations for active media, it is good to pause for a moment to stress that in a system at equilibrium, flocking would not happen in two dimensions. Let us show why.

Suppose we do not let the 'agents' move (we fix them in space, as $v_0 = 0$), but update their orientation angles θ_i according to (9.1). Rather than a model for flying birds, we now have a stochastic spin model of the type familiar from equilibrium physics. Indeed, the update rule of our fixed agents is reminiscent of relaxational dynamics of spins, where at each time step the orientation of each angle is driven toward the average orientation of the spin

and its neighbors. In addition the update rule is affected by noise. On a regular two-dimensional lattice with spacing a, this update rule is in fact the discrete form of a noisy diffusion equation,

$$\partial_t \theta = D\nabla^2\theta + \eta(\vec{r},t), \quad \left(D = \frac{a^2}{5}\right), \tag{9.4}$$

where $\eta(\vec{r},t)$ denotes white noise with zero mean and D the diffusion constant. Let us now suppose there is orientational order of these spins and that one of the spins gets oriented in a sufficiently different direction θ_0. What are the consequences of introducing this 'error' within the static version of the Vicsek model? According to (9.4) the angular variables are given by a noisy diffusion equation, with the dynamics causing angles to spread diffusively in time over a distance (see section 3.3.4 on diffusion)

$$r \sim \sqrt{t}. \tag{9.5}$$

In the absence of noise the total angle θ is conserved according to (9.4), meaning that any error or fluctuation will slowly spread out across the system. For an initial error θ_0, at time t $N(t)$ spins will be affected. In d dimensions, we then have

$$N(t) \sim r(t)^d \sim t^{d/2}. \tag{9.6}$$

As the error profile spreads out as a Gaussian, the typical size of the error $\Delta\theta(t)$ of the affected spins is of order

$$\Delta\theta(t) \simeq \frac{\theta_0}{N(t)} \sim \frac{\theta_0}{t^{d/2}}. \tag{9.7}$$

From this analysis we conclude that if a local perturbation is introduced to agents which were originally ordered, in the absence of noise, the error decays so the order is reestablished as $\Delta\theta(t) \to 0$. We now ask ourselves whether the buildup of perturbations due to the noise term in equation (9.4) can overcome this decay of errors—i.e., lead to $\Delta\theta$ growing in time—if so, we interpret this to imply that the fluctuations destroy the orientational order and hence prevent the emergence of a flock.

The noise η on a given spin will spread to others as time progresses. In fact a typical spin will accumulate $t \sim r^2$ errors, and the total collection of spins affected will accumulate a total of $N(t)t \sim r^{d+2}$ errors during this time. Now, because of the law of large numbers, the width of the distribution of angles, which gives the magnitude of the typical deviation of the spin angle from the average value, is

$$\sqrt{\langle(\Delta\theta)^2\rangle} \simeq \frac{\sqrt{\text{total errors}}}{N(t)} \sim \frac{\sqrt{r^{d+2}}}{r^d} \sim r^{1-d/2}, \tag{9.8}$$

The derivation, which is similar to the derivation of a finite-difference method for solving Laplace's equation $\nabla^2\phi = 0$ in electrostatics, is presented as problem 9.1. Of course, diffusion-type spreading of the angular variables is not limited to regular lattices, but on a disordered lattice the effective diffusion coefficient will depend on the local lattice connectivity.

The diffusion equation (9.4) implies that the error spreads out as a Gaussian; see section 3.3.4.

which diverges for $d < 2$. This means that for low dimensions, any amount of noise is sufficient to make the spins lose order completely for large enough systems. In $d = 2$, it can be shown that $\sqrt{\langle\theta^2\rangle} \sim \sqrt{\ln r} \to \infty$ for a large system, meaning fluctuations will diverge for any $d \leq 2$. In d>2, though, the static version of the Vicsek model with noise can sustain the order of the spins.

This analysis, which is a back-of-the-envelope derivation of a general statistical-mechanics result known as the Mermin-Wagner theorem, suggests that the emergence of flocks in two-dimensional computer simulations comes from the non-equilibrium character of the model.

The Mermin-Wagner theorem proves that in equilibrium vector spin models, where the spins can assume a continuum of orientations, this continuum symmetry cannot be broken at finite temperatures in two dimensions.[7] Note that Hamiltonian models of self-propelled particles have been recently introduced (Bore et al., 2016) for which the Mermin-Wagner theorem does hold (Tasaki, 2020). Hence, self-propulsion alone is not enough to induce long-range order in two dimensions.

9.2.3 Toner-Tu theory

We saw in section 9.2.1 that flocking does happen in simulations of the two-dimensional Vicsek model, and that the fact this happens is intimately related to the out-of-equilibrium character of fluids composed of self-propelled particles or birds. How should we modify the familiar hydrodynamic equations derived for passive fluids to account for this effect? The Toner-Tu theory introduces a suitable continuum model to account for the collective flocking behavior observed in the Vicsek model. We discuss it here, since the approach also provides a nice introduction to continuum modeling of active media.

The Toner-Tu approach goes back to the work by Toner and Tu, 1995. See the reviews by Toner et al., 2005 and Marchetti et al., 2013 for more extensive discussions and overviews of these types of models.

In the Vicsek flocking model, neither energy nor momentum is conserved as a result of the birds' self-propulsion—momentum is not conserved since the particles have a constant speed relative to a fixed frame. As a result, the updating rule does not conserve momentum. The only conserved quantity is the number of birds, so the hydrodynamic equations will describe the evolution of their number density ρ. Associated with the orientation of the particles is the coarse-grained local polarization field $\vec{p}$: the direction of the vector $\vec{p}$ gives the mean propagation direction of the agents, while the norm $|\vec{p}|$ measures the magnitude of the local polarization. $\vec{p}$ will be the hydrodynamic variable related to broken rotational invariance; we will discuss the significance of this in more detail later in this section. As the particles are self-propelled, the velocity field is proportional to the polarization, $\vec{v}(\vec{r}, t) = v_0\vec{p}(\vec{r}, t)$.

Both ρ and $\vec{p}$ are obtained by coarse-graining the microscopic description of the flock described by the Vicsek model. If we define the position and local orientation vector of particle i as $\vec{r}_i$ and $\hat{m}_i = [\cos\theta_i, \sin\theta_i]$,[8] respectively, ρ and $\vec{p}$ are given by

$$\rho(\vec{r}, t) = \sum_i \delta(\vec{r} - \vec{r}_i(t)),$$

$$\vec{p}(\vec{r}, t) = \frac{1}{\rho(\vec{r}, t)} \sum_i \hat{m}_i(t)\delta(\vec{r} - \vec{r}_i(t)).$$

In the Toner-Tu approach, the evolution of the coarse-grained fields $\rho(\vec{r}, t)$ and $\vec{v}(\vec{r}, t)$ is governed by a set of hydrodynamic equations whose form can be derived using symmetries and conservation laws. The Toner-Tu equations have the following form:

$$\begin{aligned} \partial_t\rho + \vec{\nabla}\cdot(\rho\vec{v}) &= 0, \\ \partial_t\vec{v} + \lambda_1(\vec{v}\cdot\vec{\nabla})\vec{v} &= -\vec{\nabla}P + \eta\nabla^2\vec{v} + \alpha\vec{v} - \beta|\vec{v}|^2\vec{v}, \end{aligned} \tag{9.9}$$

This is a compact formulation of the Toner-Tu theory. A more complete version is given in Toner et al., 2005. See problem 9.2 for a derivation of the Toner-Tu equations from the Vicsek model.

where λ_1 is a phenomenological parameter, P is the pressure, and η is a viscosity term that originates from the noise in the Vicsek model. The first relation is a continuity equation for the density of particles. The second equation can be thought of heuristically as being composed of two ingredients. The first four terms are essentially what we would expect from the Navier-Stokes equation, while the remaining terms, which read

$$\partial_t \vec{v} = \alpha \vec{v} - \beta |\vec{v}|^2 \vec{v}, \tag{9.10}$$

account for the propensity of the system to acquire a common orientation or velocity $\vec{v}$ through a pitchfork bifurcation (see section 8.2.1). The stationary states of this simple dynamical system correspond to a minimum of an effective potential density $\mathcal{F}_v$ of the form

$$\mathcal{F}_v = -\tfrac{1}{2}\alpha |\vec{v}|^2 + \tfrac{1}{4}\beta |\vec{v}|^4, \tag{9.11}$$

allowing us to write equation (9.10) as

$$\partial_t \vec{v} = -\frac{\partial \mathcal{F}_v}{\partial \vec{v}}. \tag{9.12}$$

In figure 9.5 we plot $\mathcal{F}_v$, with $\beta > 0$ to ensure that the velocity remains finite. The potential is parabolic for $\alpha < 0$ and takes the familiar bottom shape of a wine bottle for $\alpha > 0$. To understand what this means for our hydrodynamic approach, consider the net average propagation speed (or magnitude of the 'polarizatation' $|\vec{p}|$) of the birds. When $\alpha < 0$, the free energy is minimized for $\vec{v} = 0$, corresponding to the situation without any net polarization, or, equivalently, a zero mean velocity of the particles because all orientations are equally likely. This is the non-flocking phase.

When $\alpha > 0$, the disordered phase corresponding to $\vec{v} = 0$ is unstable. The lowest energy configuration occurs at any polarization $\vec{v}$ such that $v = \sqrt{\alpha/\beta}$, corresponding to the case in which the agents align with some finite mean velocity. This is the flocking state within the phenomenological description, and within this approach $\alpha = 0$ marks the flocking transition.

There are in fact infinitely many equivalent directions along which the birds could orient. The collective alignment of the flock along one chosen direction is an example of spontaneous rotational symmetry breaking. The hydrodynamic equations are invariant under rotations but their steady-state solution is not.

The Toner-Tu theory presented in this section generalizes the familiar Navier-Stokes equations of simple fluids to fluids of self-propelled particles. It allows us, for instance, to account for their flow in confined geometries as well as their sound propagation within a swarm—see problems 9.3–9.5.

We saw in section 1.9—see the note in the margin of equation (1.49)—that Galilean invariance requires $\lambda_1 = 1$ in the Navier-Stokes equation. Active matter is not Galilean-invariant, since the agents move with a well-defined speed relative to a fixed background frame (the air for birds, water for fish). Hence, for active media, $\lambda_1 \neq 1$. Note also that in this chapter we write the pressure as P rather than as p, in order to distinguish it from the polarization.

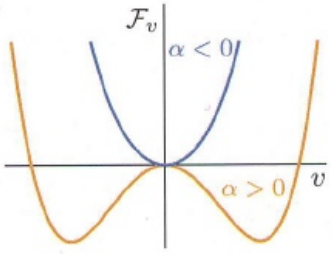

Figure 9.5. The effective potential $\mathcal{F}_v$ in the Toner-Tu theory (9.11) for different values of α. For $\alpha < 0$ (blue) F_p has a stable minimum at $v = 0$, which corresponds to the disordered phase. For $\alpha > 0$ (yellow) the curve has stable minima at $v \neq 0$, indicating alignment at finite polarization. Compare to figure 2.19.

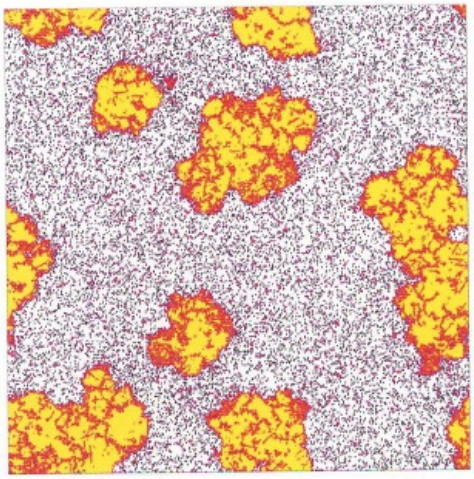

Figure 9.6. Simulations of self-propelled particles interacting via a pairwise Lennard-Jones radial potential in a periodic domain in simulations by Martin et al., 2021b.[9] The snapshot shows the occurrence of motility-induced phase separation. The two average densities corresponding to the dense and dilute clusters ($\rho_0 = 0.9$ and $\rho_0 = 0.5$) are indicated in yellow and pink, respectively.

For a review of motility-induced phase separation, see Cates and Tailleur, 2015.

The mechanism of motility-induced phase separation is reminiscent of traffic jams on highways: for sufficiently high density of cars ρ, the average driving speed $v(\rho)$ decreases with density, $\partial v/\partial\rho < 0$. This behavior of $v(\rho)$ shares some similarities with that leading to the formation of shocks, fronts, and domains in the nonlinear wave equation $\partial_t\rho + \partial_x[v(\rho)\rho] = D\partial_x^2\rho$, which is a simplified model for phenomena like traffic flows; see, e.g., Whitham, 1974. In the regime $\partial v/\partial\rho < 0$, traffic is prone to the spontaneous emergence of traffic jams due to variations ('fluctuations') in the speeds of individual cars.

9.3 Motility-induced phase separation

Motility-induced phase separation is a manifestation of the phenomenology of self-propelled particles that, unlike flocking, does not necessitate the presence of interactions that align the (flight) orientation of individual particles or agents. In essence this phenomenon relies on two ingredients.

First, particles naturally accumulate where the position-dependent propulsion speed $v(\vec{r})$ is low. Second, the self-propulsion speed $v(\vec{r})$ decreases with the local density $\rho(\vec{r})$, i.e., $\frac{\partial v}{\partial \rho} < 0$. Once these two conditions are met, a feedback loop is created that makes a uniform suspension unstable. Instead, a phase-separated state emerges in which a dilute active gas coexists with a dense liquid with reduced motility; see figure 9.6.

9.3.1 Active Brownian particles

Motility-induced phase separation happens quite generally, but it is instructive to consider a concrete model of self-propelled particles that, unlike the Vicsek model, does not display orientation-aligning interactions. In this model, self-propelled particles, called active Brownian particles, satisfy the following Langevin dynamics:

$$\dot{\vec{r}}(t) = v(\vec{r}(t))\hat{m}(\theta(t)), \qquad \dot{\theta}(t) = \sqrt{2D_\theta}\,\eta(t), \tag{9.13}$$

where $\vec{r}$ is the position of the particle, η is a Gaussian white noise, D_θ is the angular diffusion constant, and $\hat{m}(\theta) = [\cos\theta, \sin\theta]$ is the unitary vector with orientation θ. The corresponding Fokker-Planck equation for the probability distribution $P(\vec{r}, \theta)$ reads

$$\partial_t P(\vec{r}, \theta) = -\hat{n}(\theta) \cdot \vec{\nabla}\left[v(\vec{r})P(\vec{r}, \theta)\right] + D_\theta \partial_{\theta\theta} P(\vec{r}, \theta), \tag{9.14}$$

where $\vec{\nabla}$ denotes the spatial gradient and $\hat{n}$ is the average orientation. In simple terms, these equations describe a gas of non-interacting particles that self-propel with a position-dependent speed while the orientation angle θ of their velocity undergoes a random walk.

9.3.2 The mechanism behind the instability

To study the mechanism of instability that leads to motility-induced phase separation, we first write an approximate closed-form equation for the density,

$$\rho(\vec{r}, t) = \int \mathrm{d}\theta P(\vec{r}, \theta, t). \tag{9.15}$$

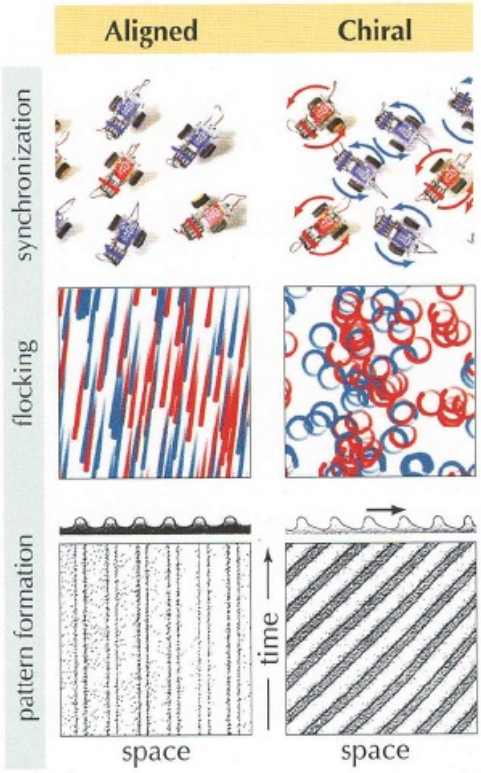

Figure 9.17. Nonreciprocal interactions between two species, R (Red) and B (Blue), induce a phase transition from static alignment to a chiral motion that spontaneously breaks parity. Top: nonreciprocal synchronization. Angular variables with nonreciprocal interactions drawn as robots spontaneously rotate either clockwise or counterclockwise, despite no average natural frequency ($\omega_m = 0$ in equation (9.63)). Middle row: non-reciprocal flocking. Self-propelled particles run in circles despite the absence of external torques. Bottom: space-time plots of an example of pattern formation with nonreciprocal interaction. A one-dimensional stationary pattern starts traveling, either to the left or to the right as in the chiral case, when nonreciprocal interactions are turned on. The figure represents an experimental observation of a moving oil-air interface (so-called viscous fingering). Adapted and reproduced with permission from Fruchart et al., 2021.[29]

incoming ones in a manner set by their spinning direction. Odd viscosity is not related to energy dissipation and, unlike standard (even) viscosity, cannot be derived from an entropy production rate equation, very much as an odd-elastic coefficient cannot be derived from variations of an elastic potential energy.

Hydrodynamic theories of active fluids capture several striking phenomena observed in experiments, including the instability shown in figure 9.16.

9.8 Nonreciprocal phase transitions

Non-equilibrium systems are typically modeled by stochastic processes that violate detailed balance. As a result, the steady states of these systems are characterized by nonvanishing probability currents between microstates, and they exhibit entropy production. A simple example is a system composed of three states with cyclic clockwise transition rates. The steady state is reached when the probabilities of being in each state are equal. This system is not at equilibrium even if it possesses a Boltzmann distribution with constant energy because it does not obey detailed balance. Similarly, physical systems with absorbing states—states out of which transitions have zero probability—clearly violate detailed balance.[30] Flocking states are a non-equilibrium example of such behavior. Nonreciprocal phase transitions describe the transitions from and to these non-equilibrium steady states.

When we discussed the flocking transition in terms of the Toner-Tu theory of section 9.2.3, we associated the transition with a pitchfork bifurcation arising from minimizing a quartic potential (see section 8.2.1 for a brief summary of the pitchfork bifurcation). The analysis of chapter 8 showed that bifurcations to time-dependent states (such as traveling waves) are typically non-potential. We now consider an example of this in active matter, in which nonreciprocal interactions lead to time-dependent phases that spontaneously break parity (mirror symmetry).[31]

9.8.1 Chiral phases in nonreciprocal active matter

We can illustrate the main features of nonreciprocal active matter with the following model:

$$\partial_t \theta_m = \omega_m + \sum_n J_{mn} \sin(\theta_n - \theta_m) + \eta_m(t), \tag{9.63}$$

which can be thought of as a simple extension of the Vicsek model. When the agents are at *fixed* positions, this model is known as the

Kuramoto model, which was introduced to study the synchronization of coupled oscillators with phase angles θ_m. It qualitatively describes the collective behavior of clocks ticking, neurons firing, or fireflies flashing.[32] With strong enough coupling, a synchronized state emerges where all oscillators evolve in phase with the same frequency.

In our case, the variable θ_m describe the angle in the plane of the velocities with which the agents move, so that the positions $\vec{r}_m$ in the plane are given by

$$\partial_t \vec{r}_m = v_0 \begin{pmatrix} \cos\theta_m \\ \sin\theta_m \end{pmatrix}. \tag{9.64}$$

An agent m tends to align with an agent n when $J_{mn} > 0$, or to antialign when $J_{mn} < 0$. The standard Vicsek flocking model corresponds to $J_{mn} > 0$. In the absence of interactions and noise the agents all rotate independently with their own frequency ω_m. For positive J_{mn}, there is a critical coupling at which a transition takes place, from incoherent rotations or motion to synchronized rotation (when the positions are fixed while $\omega_m \neq 0$) or to flocking when the particles move according to equation (9.64).

Now consider two copies of the Vicsek model describing two species, labeled 1 and 2. Without interaction between the two species, each has its own order parameter (average velocity) describing the flocking. The behavior of the model becomes especially interesting, however, when there are interactions between the species. When the interactions are reciprocal, $J_{12} = J_{21}$, we find, in addition to a disordered phase, two *static* phases where $\vec{v}_1$ and $\vec{v}_2$ are (anti)aligned, in analogy with (anti)ferromagnetism. When the interactions are nonreciprocal, $J_{12} \neq J_{21}$, a time-dependent chiral phase with no equilibrium analogue emerges between the static phases. In this chiral phase, parity is spontaneously broken: $\vec{v}_1$ and $\vec{v}_2$ (the two species are represented in red and blue in figure 9.17) rotate with a fixed relative angle $\Delta\phi$, either clockwise or counterclockwise, at a constant rotation rate $\Omega_{ss} \equiv \partial_t \bar{\phi}$, where $\bar{\phi}$ is the angle between $(\vec{v}_1 + \vec{v}_2)/2$ and a fixed direction. The chiral phase is caused by the frustration experienced by agents with opposite goals: species 1 (red) wants to align with species 2 (blue) but not vice versa. This dynamical frustration results in a 'chase and run away' motion of the order parameters $\vec{v}_1$ and $\vec{v}_2$.

Interestingly, Rayleigh-Bénard convection in rotating cells is described by a nonreciprocal model, in which the nonreciprocal effects affect the nonlinear terms describing mode interactions. See the note in the margin of equation (8.54).

Figure 9.17 illustrates the aligned-to-chiral transition in flocking as well as in synchronization and pattern formation.[33] The bottom row of the figure illustrates a strong link with the formation of patterns as discussed in chapter 8: in pattern-forming non-equilibrium systems, nonreciprocal interactions can similarly lead to a transition from stationary to moving patterns, and the methods of the theory of pattern formation and dynamical systems can be used to understand general features of the phases and phase transitions.

9.11 Problems

Relevant coding problems and solutions for this chapter can be found on the book's website www.softmatterbook.online under Chapter 9/Coding problems.

Problem 9.1 ***The Vicsek model as a noisy diffusion equation***

In this problem we illustrate how the Vicsek model (9.1) for fixed agents, i.e., $\vec{v}_i = 0$, on a two-dimensional lattice reduces to the noisy diffusion equation (9.4).

a. A sketch of the system is shown in figure 9.28, where we have represented agents as fixed spins on a square lattice. Show that the update rule (9.1) reduces in the case where $a < R < a\sqrt{2}$ to

$$\theta(\vec{r}, t+1) = \frac{1}{5}\left(\theta(\vec{r}, t) + \sum_{\Delta\vec{r}=\pm a\hat{e}_{x,y}} \theta(\vec{r}+\Delta\vec{r}, t)\right) + \eta(\vec{r}, t), \tag{9.82}$$

where the sum runs over all four near neighbor lattice directions and the vector $\vec{r}$ marks the lattice points.

b. Make the assumption that $\theta(\vec{r}, t)$ varies smoothly as a function of space and time, and perform an expansion to lowest order in the gradients. Show that this leads to equation (9.4) with a diffusion coefficient $D = a^2/5$.

c. You may wonder why truncating the above expansion to the lowest order in the gradients is justified. Compare with problem 3.4 part d, and argue that the above procedure does give the exact asymptotic long time diffusion result.

d. Consider the case in which $\sqrt{2}a < R < 2a$ and show that this gives the diffusion constant $D = a^2/3$.

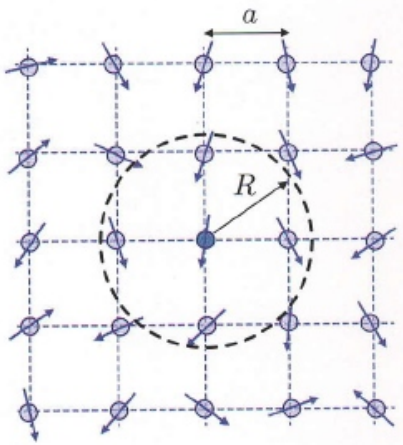

Figure 9.28. The Vicsek model on a square lattice with agents (spins) fixed on the lattice sites. The circle of radius R marks the area with spins that are included in the updating of the central spin, the dark dot. As you can see, only nearest neighbors are included in the updating in the case drawn.

Problem 9.2** ***The Dean equation: Coarse-graining the Vicsek model to obtain Toner-Tu equations***

In problem 3.10 we discussed the Dean equation for fluctuating variables. In this problem we show how the method can be used to derive the coarse-grained Toner-Tu equations from the Vicsek model. Let us consider N active particles moving in a plane. Each particle is described by a position r_i and an angle θ_i, with $i = 1, \ldots, N$. The dynamics of the population is described by the set of equations

This problem is an application of the analysis by Dean discussed in problem 3.10.

$$\dot{\vec{r}}_i(t) = v_0 \hat{n}[\theta_i(t)], \tag{9.83}$$

$$\dot{\theta}_i(t) = \eta_i(t) + \sum_{j=1}^{N} J_{ij} \sin[\theta_j(t) - \theta_i(t)], \tag{9.84}$$

where

$$\hat{n}(\theta) = (\cos(\theta), \sin(\theta))^T \tag{9.85}$$

gives the local orientation of the agent, and $\eta_i(t)$ are Gaussian white noises with $\langle \eta_i(t) \rangle = 0$ and